Journal of Statistical Physics, Vol. 111, Nos. 5/6, June 2003 (© 2003)

Ensemble Dynamics of Intermittency and Power-Law Decay

Kevin Nelson[1] **and Dean J. Driebe**[1, 2]

Received January 5, 2001; accepted October 11, 2002

A spectral decomposition of the Frobenius–Perron operator is constructed for one-dimensional maps with intermittent chaos, using the method of coherent states. A technique using the spectral density function is applied to the the well-known cusp map, which generates weak type-II intermittency. Higher-order corrections are obtained to the leading $1/t$ long-time behavior of the $x-x$ autocorrelation.

KEY WORDS: Intermittency; power-law decay; $1/f$ noise; cusp map; Frobenius–Perron operator.

1. INTRODUCTION

The ubiquity of power-law distributions and $1/f$ noise in nature is now well-recognized.[1] Among the mechanisms generating such distributions are self-organized criticality[2], chaotic transport with Lévy flights[3] and intermittency.[4] The usual theoretical description of these phenomena is concerned with the statistics of important observables, such as the $x-x$ autocorrelation function.[5] Typical analyses concentrate on trajectory dynamics and calculate statistical quantities such as the average length of the laminar regions of time series in systems with intermittent chaos.

Our approach to intermittent chaos does not look at trajectories; rather, we concentrate on the evolution of probability densities governed by the Frobenius–Perron operator.[6] A spectral decomposition of this linear operator gives a complete solution of the statistical evolution of the system. Such complete decompositions have been constructed for a variety of fully chaotic systems in recent years.[7–9]

[1] Center for Studies in Statistical Mechanics and Complex Systems, The University of Texas, Austin, Texas 78712; e-mail: dean@physics.utexas.edu

[2] International Solvay Institutes for Physics and Chemistry, 1050 Brussels, Belgium.

0022-4715/03/0600-1183/0 © 2003 Plenum Publishing Corporation

In fully chaotic systems with exponential approach to equilibrium there exist discrete decay modes.[10] Techniques for calculating these modes are not directly amenable to the marginal chaos of intermittent systems, where there is power-law approach to equilibrium. As is well known though, power-law behavior may be obtained from a continuous superposition of exponential decay modes.[1, 4, 11]

We will show how to construct such modes explicitly for a general class of maps and then we will apply our method to the cusp map. The method is similar to previous discussions of the continuous spectrum associated with fully chaotic systems.[12] It starts with the construction of shift states of the Frobenius–Perron operator from which eigenstates,[3] sometimes called coherent states, are constructed. General densities and observables may then be expressed as a continuous superposition of these coherent states.

Other authors have considered the statistical dynamics of intermittency through an analysis of the Frobenius–Perron operator. Hasegawa and Luschei[13] calculated the power spectrum of the Manneville–Pomeau map through a spectral analysis associated with a piecewise-linear version of the map. Kaufmann *et al.*[14] calculated eigenmodes for a family of maps whose limiting parameter value yielded the cusp map that is considered in the present paper. Their matrix representation method was unable to obtain eigenstates for the cusp map, whereas our coherent state construction does obtain them.

In the next section our general approach is described. We then turn in the following section to the application of the method to the cusp map. Using special properties of intermittent maps we construct smooth eigenfunctions associated with the continuous spectrum of the Frobenius–Perron operator of the cusp map. This spectral decomposition is then applied to calculate the $x-x$ autocorrelation function. The well-known power-law behavior in time of this function[15] is recovered as well as corrections to the leading-order result.

2. GENERAL METHOD

For a system with discrete-time trajectory dynamics given by $x_{t+1} = f(x_t)$ a probability density ρ on the phase space M evolves as

$$\rho(x, t+1) = U\rho(x, t) \equiv \int_M dx'\, \delta(x - f(x'))\, \rho(x', t) \tag{1}$$

[3] Since these states are associated with a continuous spectrum they may be referred to as quasi-eigenstates or generalized eigenstates. We will not use the qualifier "generalized" for them because that terminology is used in related work for eigenstates that are generalized functions.

where the linear operator U is the Frobenius–Perron operator of the system.[6, 7]

We will construct spectral decompositions of the Frobenius–Perron operator using the technique of coherent states.[7, 12] The first step is to obtain a complete set of shift states of U. We denote the shift states by $e_{n,s}$ where n is a nonnegative integer and s is an index whose range will depend on the system in question. The shift states satisfy

$$Ue_{n,s} = \begin{cases} 0, & n = 0 \\ e_{n-1,s}, & n \geqslant 1 \end{cases} \tag{2}$$

The full set of states can be constructed by starting with a set of states in the kernel of U, i.e.,

$$Ue_{0,s} = 0 \tag{3}$$

which we sometimes refer to as the seed functions of the construction. For maps that preserve probability these seed functions necessarily carry zero probability.

We now assume that U has a right inverse U_R^{-1}, which is equivalent to assuming that the range of f is the entire phase space. (Note however that U_R^{-1} will be non-unique if f is non-invertible). We use the right inverse U_R^{-1} to obtain the full set of shift states as

$$e_{n,s} = U_R^{-n} e_{0,s} \tag{4}$$

These states inherit the zero probability property of the seed functions so that the full set spans a space orthogonal to the invariant probability density.

Using the shift states the coherent eigenstates are given by

$$\phi_{z,s} = \sum_{n=0}^{\infty} z^n e_{n,s} \tag{5}$$

The spectrum of U in this representation is then the set of values of z for which the series (5) converges.

In order to expand a given density ρ in terms of the coherent states we use their dual states.[4] We use the following bilinear form between functions on the unit interval:

$$\langle A \mid \rho \rangle \equiv \int_0^1 A^*(x)\, \rho(x)\, dx \tag{6}$$

[4] Since the Frobenius–Perron operator may also be used in the context of correlation functions to evolve observables, the "density" that we speak of is not necessarily a non-negative function with unit norm. We will however assume that $\rho \in L^1$.

The left states $\langle \tilde{e}_{m,r}|$ dual to the shift states $e_{n,s}$ satisfy

$$\langle \tilde{e}_{m,r} \mid e_{n,s} \rangle = \delta_{mn}\delta_{rs} \tag{7}$$

where r and s are integers.

The expansion of a density $\rho(x)$ in terms of the shift states is then

$$\rho(x) = \rho^{\text{eq}}(x) + \sum_{s=1}^{\infty} \sum_{n=0}^{\infty} b_{n,s} e_{n,s}(x) \tag{8}$$

where $b_{n,s} = \langle \tilde{e}_{n,s} \mid \rho \rangle$. The expansion of $\rho(x)$ in terms of the coherent states is

$$\rho(x) = \rho^{\text{eq}}(x) + \sum_{s=1}^{\infty} \frac{1}{2\pi i} \oint_{|z|=1} dz\, \phi_{z,s}(x) \langle \tilde{\phi}_{z,s} \mid \rho \rangle \tag{9}$$

The contour is chosen to enclose all decaying eigenvalues. Those z lying exactly on the contour can be ignored, since for them $\phi_{z,s}(x)$ is either not defined or not L^1. The assumption that $\rho(x) \in L^1$, together with the fact that the $\phi_{z,s}(x)$ are linearly independent, means that the $\phi_{z,s}(x)$ with $|z| = 1$ cannot contribute to $\rho(x)$.

The dual coherent states $\tilde{\phi}_{z,s}(x)$ may be obtained[12] from the dual shift states as:

$$\tilde{\phi}_{z,s}(x) = \sum_{n=0}^{\infty} (z^*)^{-(n+1)}\, \tilde{e}_{n,r}(x) \tag{10}$$

These states satisfy:

$$\langle \tilde{\phi}_{z',r} \mid \phi_{z,s} \rangle = \frac{\delta_{rs}}{z - z'} \tag{11}$$

a relation that is necessary so (9) will hold.

The spectral density function

$$\beta_s(z) \equiv \langle \tilde{\phi}_{z,s} \mid \rho \rangle \tag{12}$$

appearing in (9) describes the expansion of a given density $\rho(x)$ over the coherent states. In can be calculated analytically in some cases[12] but must be obtained numerically in general. Since the time evolution of a density is given by

$$\rho(x,t) = U^t \rho(x,0) = \rho^{\text{eq}}(x) + \sum_{s=1}^{\infty} \frac{1}{2\pi i} \oint_{|z|=1} z^t \beta_s(z)\, \phi_{z,s}(x)\, dz \tag{13}$$

the analytic structure of $\beta_s(z)$ determines the time evolution of $\rho(x)$.

We now specialize to the case of a one-dimensional map on the unit interval. Let its branches be indexed by i, and denote as L_i the domain of the ith branch. In this paper only maps for which each branch has full height (i.e., a range of [0, 1]) are considered. The action of the Frobenius–Perron operator of the map is given by

$$U\rho(x) = \sum_i \frac{\rho[f_i^{-1}(x)]}{|f'[f_i^{-1}(x)]|} \tag{14}$$

where i runs over the total number of branches.

Associated with each branch we define the operator U_i^{-1}, which is a right inverse for the complete U, as

$$U_i^{-1}\rho(x) = \begin{cases} \dfrac{\rho[f(x)]}{|f_i^{-1\prime}[f(x)]|}, & x \in L_i \\ 0, & \text{otherwise} \end{cases} \tag{15}$$

The effect of U_i^{-1} on $\rho(x)$ is to compress it (in general non-uniformly) into the subinterval L_i and then to rescale it. If U_i^{-1} is applied repeatedly, then the resulting function will have its support squeezed into a smaller and smaller interval, but the L_1 norm will be preserved.

We can obtain more right inverses, to be called as a general term U_c^{-1}, by taking linear combinations of the U_i^{-1}:

$$U_c^{-1} = \sum_i c_i U_i^{-1} \tag{16}$$

subject to the condition $\sum_i c_i = 1$. Later we will impose a smoothness condition that will require a particular choice of c_i coefficients.

3. NONEQUILIBRIUM DYNAMICS OF THE CUSP MAP

Now we apply the coherent state expansion of the Frobenius–Perron operator to the case of a map with intermittent behavior having power-law decay of typical observables and time correlation functions. Although we are concentrating specifically on the cusp map, the techniques used are also applicable to other one-dimensional maps with intermittency caused by a marginal fixed point (for example, the Farey map[17] or the Manneville–Pomeau map[4]).

The cusp map on the unit interval, [0, 1), is defined by the rule

$$f(x) = 1 - \sqrt{|2x-1|} \tag{17}$$

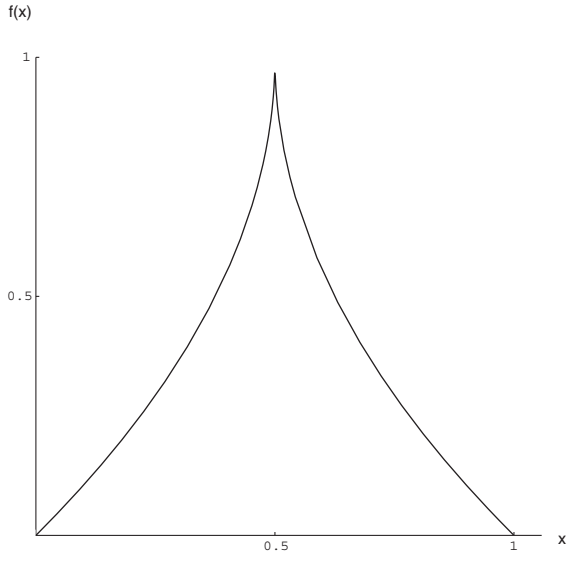

Fig. 1. The cusp map, $f(x) = 1 - \sqrt{|2x-1|}$.

A graph of this function is shown in Fig. 1. It is of interest in several physical situations; most notably, it is an approximate return map for the Lorenz system with certain parameters. The map shows type-II intermittency[5] with a marginally stable fixed point at $x = 0$. A trajectory near this fixed point moves away from it very slowly.

The Frobenius–Perron operator of the cusp map is given by

$$U\rho(x) = (1-x)[\rho(f_0^{-1}(x)) + \rho(f_1^{-1}(x))] \tag{18}$$

where $f_0^{-1}(x)$ and $f_1^{-1}(x)$ are the two right inverses of f, one for each branch:

$$\begin{aligned} f_0^{-1}(x) &= \tfrac{1}{2} - \tfrac{1}{2}(1-x)^2 \\ f_1^{-1}(x) &= \tfrac{1}{2} + \tfrac{1}{2}(1-x)^2 \end{aligned} \tag{19}$$

The stationary eigenstate of U, corresponding to the equilibrium density, is[18]:

$$\rho^{\text{eq}}(x) = 2(1-x) \tag{20}$$

The equilibrium density is regular at the marginal fixed point at $x = 0$, so the cusp map is classified as having weak intermittency.

Note that U in (18) annihilates any function odd around $x = 1/2$. A convenient set of seed functions is

$$e_{0,s}(x) = \sqrt{2}\cos[(2s-1)\,\pi x] \tag{21}$$

where $s \geqslant 1$. (The factor of $\sqrt{2}$ is chosen so that the set is orthonormal, i.e., $\langle e_{0,s} \mid e_{0,s'} \rangle = \delta_{ss'}$)

The right inverses of U associated with each branch of the map are

$$U_0^{-1}\rho(x) = \begin{cases} \dfrac{\rho(f(x))}{\sqrt{|2x-1|}}, & 0 \leqslant x \leqslant 1/2 \\ 0, & 1/2 < x \leqslant 1 \end{cases} \tag{22}$$

$$U_1^{-1}\rho(x) = \begin{cases} 0, & 0 \leqslant x < 1/2 \\ \dfrac{\rho(f(x))}{\sqrt{|2x-1|}}, & 1/2 \leqslant x \leqslant 1 \end{cases} \tag{23}$$

These right inverses can be combined to form other right inverses as in (16), e.g.

$$U_{(01)}^{-1} = \tfrac{1}{2}(U_0^{-1} + U_1^{-1}) \tag{24}$$

One set of shift states will then be given by

$$e_{n,s}(x) = U_{(01)}^{-n} e_{0,s}(x) \tag{25}$$

The action of $U_{(01)}^{-1}$ on a function creates two compressed copies of the original function, one on each half-interval.

Using the above shift states, definition (5) for $\phi_{z,s}(x)$ converges for any z in the complex unit disk. However, the $\phi_{z,s}(x)$ are rather irregular. That is because the $e_{n,s}$ rapidly become more oscillatory, with the number of oscillations increasing exponentially with n. For $z \neq 0$ the $\phi_{z,s}(x)$ are not infinitely differentiable. In general, they are relatively smooth for $|z| \approx 0$ and they become more irregular as $|z|$ increases towards 1. It is more natural though to expand a smooth $\rho(x)$ over smooth basis states. We now turn to the construction of smooth coherent states.

3.1. Smooth Coherent States of the Cusp Map

As discussed above, we have a great deal of freedom in choosing right inverses U_c^{-1} for U. By choosing $U_c^{-1} = U_0^{-1}$, we can create smooth coherent states. Once the existence of those states is demonstrated, conclusions about the spectrum of U will follow.

The operator U_0^{-1} corresponding to the branch containing the marginal fixed point produces, when acting successively, relatively weak compression of functions. It thus produces shift states and coherent states with less pronounced oscillation.

We start by modifying the seed functions in (21) by tempering them as

$$g_{0,s}(x) = e_{0,s}(\alpha(x))\,\alpha'(x) \tag{26}$$

where $\alpha(x)$ is an infinitely differentiable, one-to-one function from $[0, 1)$ onto $[0, 1)$. We require $\alpha(x)$ to satisfy the following three conditions: $\alpha(1-x) = 1-\alpha(x)$; *all* derivatives of $\alpha(x)$ vanish at $x = 0$ and $x = 1$; and $\alpha(0) = 0$. The first condition is necessary to ensure that $g_{0,s}(x)$ is odd around $x = 1/2$ and hence that $Ug_{0,s}(x) = 0$. The second condition will wind up ensuring the smoothness of the coherent states constructed from the $g_{n,s}(x)$. The third condition ensures a fairly close relationship between $g_{0,s}(x)$ and $e_{0,s}(x)$, reminiscent of topological conjugacy, and makes the completeness of the $g_{n,s}(x)$ easier to show.

With an $\alpha(x)$ satisfying the above conditions, all derivatives of $g_{0,s}(x)$ are 0 at the endpoints of the unit interval. Now using $U_c^{-1} = U_0^{-1}$ we get the shift states

$$g_{n,s}(x) = U_0^{-n} g_{0,s}(x) \tag{27}$$

which are infinitely differentiable. In terms of the c_i coefficients discussed in Section 2, we are simply choosing $c_0 = 1$ and $c_1 = 0$. The effect of U_0^{-n} is to compress $g_{0,s}(x)$ into a small subinterval at the left end of the unit interval. Since the fixed point at $x = 0$ is marginal, U_0^{-1} produces only very slow compression; the $g_{n,s}(x)$ become more compressed as n increases, but only very slowly. That will turn out to be a key fact. Because $g_{0,s}(x)$ started out with all its derivatives equal to 0 at $x = 1$, even after the compression it joins smoothly with the rest of the unit interval, where $g_{n,s}(x) = 0$. Also note that all the $g_{n,s}(x)$ have all derivatives equal to 0 at $x = 0$, a fact that will come in useful later.

Several of these $g_{n,s}(x)$ are shown in Fig. 2, where the specific $\alpha(x)$ chosen is

$$\alpha(x) = \frac{1}{2}\tanh\left\{\tan\left[(2x-1)\frac{\pi}{2}\right]\right\} + \frac{1}{2} \tag{28}$$

(This $\alpha(x)$ may seem rather complicated, but it was chosen as perhaps the simplest function satisfying the necessary conditions.) It may appear from the graphs that there is a discontinuity in the first derivative of some of the

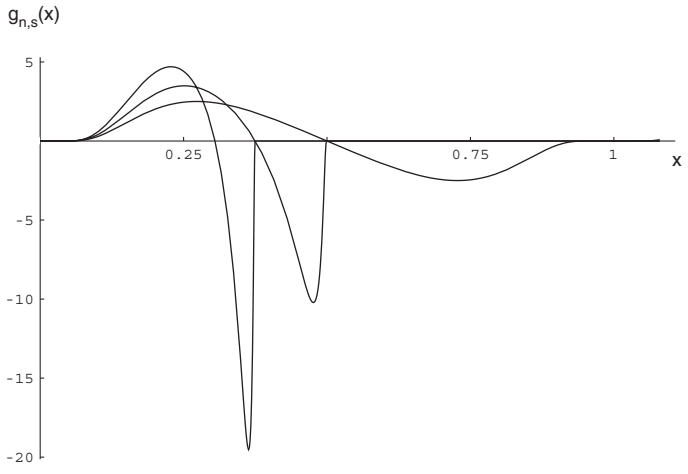

Fig. 2. The tempererd shift states $g_{0,1}(x)$, $g_{1,1}(x)$, and $g_{2,1}(x)$. These functions become compressed more and more towards the left end of the unit interval as n (the first index) becomes larger.

$g_{n,s}(x)$, but if the graphs were made with sufficient magnification the functions would all look smooth.

Coherent states $\psi_{z,s}(x)$ can be constructed based on the above shift states just as before:

$$\psi_{z,s}(x) = \sum_{n=0}^{\infty} z^n g_{n,s}(x) \tag{29}$$

One of them is shown in Fig. 3. In contrast to the coherent states constructed in the previous section the $\psi_{z,s}(x)$ are infinitely differentiable. For $x > 0$, that can be seen almost immediately. Only a finite number of terms in the sum $\sum_{n=0}^{\infty} z^n g_{n,s}(x)$ will have support in a neighborhood of x. As n gets larger the support of $g_{n,s}(x)$ gets more compressed into the left end of the unit interval. For large enough n, the support of $g_{n,s}(x)$ will be compressed to the left of any given x if $x > 0$. The sum in (29) then becomes a finite one. It immediately follows that $\psi_{z,s}(x)$ is infinitely differentiable for $x > 0$.

The function $\psi_{s,z}(x)$ is also infinitely differentiable with respect to x at $x = 0$, though the reason is less obvious. Ultimately it is due to the slow compression of the $g_{n,s}(x)$ as n increases. That can be seen as follows.

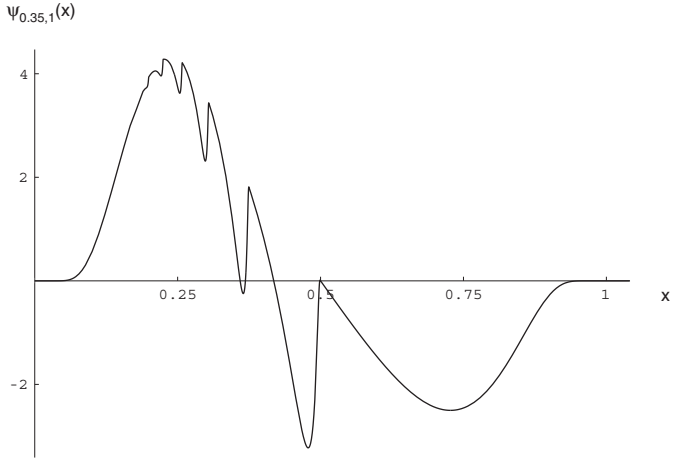

Fig. 3. The smooth coherent state $\psi_{0.35,1}(x)$. This function is infinitely differentiable, though that may not be apparent from looking at the graph.

First note that

$$\begin{aligned} g_{n,s}(x) &= U_0^{-n+1} U_0^{-1} g_{0,s}(x) \\ &= U_0^{-n+1} \left[\frac{1}{\sqrt{|1-2x|}} g_{0,s}(f(x)) \right] \\ &= U_0^{-n+2} \left[\frac{1}{\sqrt{|1-2x|}} \frac{1}{\sqrt{|1-2f(x)|}} g_{0,s}(f^2(x)) \right] \\ &= \frac{1}{\sqrt{|1-2x|}} \frac{1}{\sqrt{|1-2f(x)|}} \cdots \frac{1}{\sqrt{|1-2f^{n-1}(x)|}} g_{0,s}(f^n(x)) \end{aligned} \tag{30}$$

Replacing x above by $f_0^{-n}(x)$, we get

$$\begin{aligned} & g_{n,s}(f_0^{-n}(x)) \\ &= \frac{1}{\sqrt{1-2f_0^{-n}(x)}} \frac{1}{\sqrt{1-2f_0^{-n+1}(x)}} \cdots \frac{1}{\sqrt{1-2f_0^{-1}(x)}} \frac{1}{\sqrt{|1-2x|}} g_{0,s}(x) \\ &\approx \frac{n+1}{n} \frac{n}{n-1} \cdots \frac{1}{\sqrt{|1-2x|}} g_{0,s}(x) \end{aligned} \tag{31}$$

where the second step follows because for any $x \in (0, 1]$, $f_0^{-n}(x) \propto 1/n$ for large n.[15] So the above expression increases with at most a power-law dependence on n; and furthermore, there is some $a > 1$ such that $g_{n,s}(f_0^{-n}(x))$ grows slower than n^a for all x.

One can differentiate (31) an arbitrary number of times with respect to its argument, and still there will only be a sum of terms that have a power-law growth with respect to n (and with a bounded exponent).

It is already known that $g_{n,s}^{(m)}(0) = 0$, where $g_{n,s}^{(m)}(x)$ is the mth derivative of $g_{n,s}(x)$. It follows that

$$\sup_{x \in [0,1]} |g_{n,s}^{(m)}(x)| = \sup_{x \in [0,1]} |g_{n,s}^{(m)}(f_0^{-n}(x))| \tag{32}$$

grows with at most a power-law dependence on n. Then, in the expression

$$\sum_{n=0}^{\infty} z^n g_{n,s}^{(m)}(x) \tag{33}$$

the factor of z^n will force exponential decline towards 0 as $n \to \infty$. (Remember that $|z| < 1$.) The series will be uniformly convergent on [0,1]; and since $g_{n,s}^{(m)}(0) = 0$,

$$\psi_{z,s}^{(m)}(0) = \sum_{m=0}^{\infty} z^n g_{n,s}^{(m)}(0) = 0 \tag{34}$$

Clearly, the above argument will not work for non-intermittent maps. If the fixed point is expanding and hyperbolic, the prefactor associated with U will not approach 1, as it does in (31); rather, it will approach some number greater than 1, so the quantity corresponding to $g_{n,s}(f_0(x))$ will grow exponentially with n.

Hence, imposing a differentiability condition does *not* reduce the spectrum to anything less than the unit disk. That is in contrast to maps

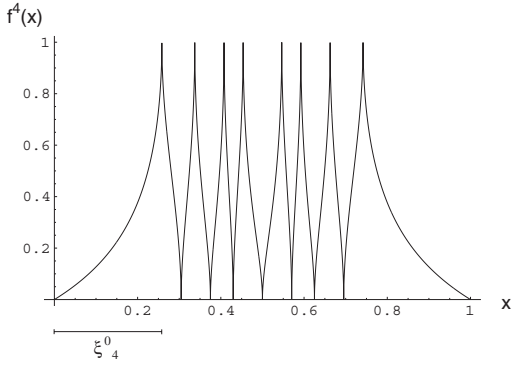

Fig. 4. The fourth iterate of the cusp map. Even for such low n, it is already clear that the domains of the first and last branches are much longer than any of the others. That reflects the slow, power-law decrease of $\xi_n^0 \equiv f_0^{-n}(1)$ with respect to n.

with fully developed chaos. Such maps have an expanding constant $q > 1$, and the essential spectral radius of U acting within $C^k[0, 1]$ is less than or equal to q^{-k}.[16] For example, the dyadic Bernoulli map has coherent states with $|z| < 1$. If U is restricted to act within the space of C^∞ functions, the essential spectral radius shrinks to zero and the only eigenvalues of U that remain are the discrete values of $z = 1/2^m$ for $m \geqslant 0$.[12]

However, as we see below, by imposing the stronger condition of analyticity on $[0, 1]$ it is possible to reduce the spectrum of U even for the cusp map.

We could now consider the expansion of a function over the coherent states $\psi_{z,s}(x)$. But it is more convenient to consider an the expansion over the shift states $g_{n,s}(x)$.

The following set of functions are dual shift states:

$$\tilde{g}^0_{0,r}(x) = \begin{cases} 0, & 0 \leqslant x < 1/2 \\ 2e_{0,r}(\alpha(x)), & 1/2 \leqslant x < 1 \end{cases} \tag{35a}$$

$$\tilde{g}^0_{m,r}(x) = K^m \tilde{g}_{0,r}(x), \qquad m \geqslant 1 \tag{35b}$$

where $K = U^\dagger$ is the Koopman operator of the cusp map given by

$$KA(x) = A(f(x)) \tag{36}$$

and $f(x)$ is the rule (17) for the map. One can see that these are duals to the shift states defined in (27) as

$$\begin{aligned} \langle \tilde{g}^0_{m,r} \mid g_{n,s} \rangle &= \langle K^m \tilde{g}^0_{0,r} \mid U_0^{-n} g_{0,s} \rangle \\ &= \langle \tilde{g}^0_{0,r} \mid U^m U_0^{-n} g_{0,s} \rangle \\ &= \delta_{rs} \delta_{mn} \end{aligned}$$

Since we are interested in the approach towards equilibrium, we will look at the density $\delta\rho(x)$ obtained by subtracting off the equilibrium component of $\rho(x)$:

$$\delta\rho(x) = \rho(x) - \rho^{\text{eq}}(x) \int_0^1 \rho(u)\, du \tag{37}$$

(Since $\rho(x)$ is not necessarily a probability density, its integral over the unit interval is not necessarily one.) The expansion of $\delta\rho(x)$ over the $g_{n,s}(x)$ will have the coefficients

$$\begin{aligned} b_{n,s} &= \langle \tilde{g}^0_{n,s} \mid \delta\rho \rangle \\ &= \int_0^1 \tilde{g}^0_{n,s}(x)\, \delta\rho(x)\, dx \end{aligned} \tag{38}$$

It turns out that for continuous $\delta\rho(x)$, the series

$$\sum_{n=0}^{\infty} \sum_{s=1}^{\infty} b_{n,s} g_{n,s}(x) \tag{39}$$

will converge pointwise to $\delta\rho(x)$ almost everywhere. More specifically, it will converge to $\delta\rho(x)$ for all $x \in [0, 1]$ except $x = 0$ and $x = \xi_n^0 \equiv f_0^{-n}(1)$ for $n \geqslant 0$. At those points the series will still converge to a finite value, so the singularities there are removable. The proof of the convergence is somewhat tedious, but straightforward. It involves splitting the unit interval into the subintervals $[\xi_{n+1}^0, \xi_n^0]$ and treating various parts of the above series as modified Fourier series within those subintervals. The convergence is non-uniform, and it is slow in the vicinity of $x = 0$ or $x = \xi_n^0$.

Certain properties of the $b_{n,s}$ (in particular, their large n dependence) can be seen more clearly if we replace $\tilde{g}_{n,s}^0(x)$ in the integral (38) by $\tilde{g}_{n,s}(x) = \tilde{g}_{n,s}^0(x) + k_{n,s}$, where $k_{n,s}$ is a constant chosen so

$$\int_0^1 \tilde{g}_{n,s}(x)\, dx = 0, \tag{40}$$

i.e.,

$$k_{n,s} = -\int_0^1 \tilde{g}_{n,s}^0(x). \tag{41}$$

Since $\delta\rho(x)$ has an average value of 0, the coefficients $b_{n,s}$ will be unaffected by the above substitution. If specific values of $k_{n,s}$ are needed, they will have to be found numerically (as is done in the Appendix). However, the necessary numerical work is lessened because for $n \geqslant 1$,

$$\begin{aligned} k_{n,s} &= -\int_0^1 K^n \tilde{g}_{0,s}^0(x)\, dx \\ &= -\int_0^1 \tilde{g}_{0,s}^0(x)\, U^n[1]\, dx \\ &= -\int_0^1 \tilde{g}_{0,s}^0(x)\, \rho^{\text{eq}}(x)\, dx \\ &= k_{1,s} \end{aligned} \tag{42}$$

(Note that we are using $U[1] = \rho^{\text{eq}}(x)$, which is a special feature of the cusp map.) One of the functions $\tilde{g}_{n,s}(x)$ is graphed in Fig. 5.

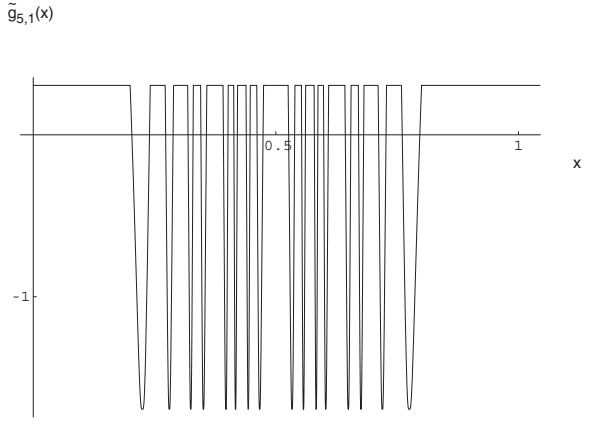

Fig. 5. The displaced dual shift state $\tilde{g}_{5,1}(x)$. This function has an average value of 0.

Let us restrict U to act within the space of densities $\rho(x)$ analytic on $[0, 1]$. In that case, f and its induced U will satsify the conditions of Theorem 1.1 in Ref. 19. One of the conclusions of the theorem is that the continuous spectrum of U is contained in [0,1], with only isolated eigenvalues elsewhere in the unit disk. We will now present a heuristic argument to the effect that there should be a branch cut all along [0,1] and no discrete isolated eigenvalues at all.

The basic idea is to look at the large-n behavior of the $b_{n,s}$ coefficients, using equation (38) and the characteristics of $\tilde{g}_{n,s}(x)$. As Fig. 5 shows, $\tilde{g}_{n,s}(x)$ is a highly oscillatory function whose domain can be divided up into 2^{n+1} segments. Each segment is a preimage of one of f's branches. For high enough n, $\rho(x)$ *within* that segment will look like a polynomial.

Since the average value of $\delta\rho(x)$ is 0 and the $\tilde{g}_{n,s}(x)$ rapidly become more oscillatory with increasing n, the integral (38) is quite difficult to evaluate numerically past the first few values of n. The function $\tilde{g}_{n,s}(x)$ has $s2^{n-1}$ oscillations, so intuitively one might expect that the $b_{n,s}$ would decrease exponentially with n. However, that is not true. The *average* oscillation in $\tilde{g}_{n,s}(x)$ has length $2^{-n+1}/s$, but some of the individual oscillations have a length that decreases with a power-law dependence on n. Most notably, the first and last segments in the unit interval have a length proportional to $1/n$, yielding a component of $b_{n,s}$ proportional to $1/n$. Other nested sequences of segments have lengths proportional to $1/n^a$ for various exponents a.

The contribution to $b_{n,s}$ from the first and last segments, as part of the integral (38), will then decrease proportionally to $1/n$. Within some segments the rate of decrease will be faster than others, but the

"slowly-decreasing" segment-sequences are densely distributed in the unit interval, so any analytic $\rho(x)$ will have the large-n behavior of its $b_{n,s}$ determined by them. The conclusion is that the $b_{n,s}$ should always have a slow, power-law decrease for large n. Since an eigenfunction of U would have the $b_{n,s}$ exponentially decreasing with n, it follows that no analytic $\rho(x)$ can be an eigenfunction of U, so U as restricted to the space of analytic functions has no isolated eigenvalues.

To deal more precisely with the continuous spectrum along $[0, 1]$, recall that $\xi_n^0 = f_0^{-n}(1)$. From the definition of $\tilde{g}_{n,s}^0(x)$ in (38) it immediately follows that the initial and final "flat" segments, where $\tilde{g}_{n,s}^0(x) = 0$ and where $\tilde{g}_{n,s}(x) = k_{n,s}$, have a length of exactly ξ_{n+1}^0. Furthermore, it is known[15] that for large n,

$$\xi_n^0 = \frac{2}{n+9} \tag{43}$$

to leading order in n. So it is clear why the first and last flat segments, which have a length that approaches $2/n$ for large n, make the dominant contribution to the integral in (38) for large n. (Clearly, there is a special case if $\rho(1) = -\rho(0)$, in which case the contribution from the last segment will cancel that from the first. In that case, higher-order effects come into play and the $b_{n,s}$ will show a faster though still power-law decay with respect to n.)

There will also be many nested sequences of smaller flat segments in the interior of the unit inverval whose length is proportional to $1/n^2$. K^m, acting on the flat segments at the ends of the unit inverval with length ξ_n^0, produces $2^m - 1$ interior flat segments each of which, for fixed n, has length proportional to $(\xi_n^0)^2$. These will result in a correction to the dominant $1/n$ behavior of $b_{n,s}$.

For intermittent maps in general, $b_{n,s}$ will show an inverse power-law dependence on n though the dominant term will not necessarily go as $1/n$. The specific case illustrated is typical of the general case: The branch of $f^n(x)$ containing the marginal fixed point will have a length that decreases with an inverse power-law dependence on n.[15] That is a key difference from fully developed chaotic maps, for which the corresponding dependence will be an exponential decrease in n.

For the cusp map, based on the fact that $b_{n,s} \propto 1/n$ for large n, one can decompose $b_{n,s}$ into various components. The dominant component is exactly proportional to $1/n$ for all n. The other components will decay faster than $1/n$. Correspondingly,

$$\beta_s(z) = \sum_{n=0}^{\infty} z^{-(n+1)} b_{n,s} \tag{44}$$

can also be divided into two components. The dominant component will be proportional to

$$\ln(1-1/z) = \sum_{n=1}^{\infty} \frac{1}{n}\frac{1}{z^n} \tag{45}$$

which has a branch cut running between branch points at 1 and 0. Note that the right-hand side is convergent only for $|z| > 1$, but it can be analytically continued in a straightforward way to the expression on the left-hand side, which is valid even for $|z| < 1$.

The entire heuristic argument presented above for the cusp map can be extended to a large class of intermittent maps, because all that is necessary is for the branch of f^n containing the marginal fixed point to have the length of its domain decrease as $1/n$. Many intermittent maps meet that condition.[15]

For the cusp map specifically, it is possible to say somewhat more. If there is a contribution to $b_{n,s}$ proportional to $1/n^k$ for real $k > 0$, then $\beta_s(z)$ will have a component proportional to

$$\mathrm{Li}_k(1/z) = \sum_{n=1}^{\infty} \frac{1}{n^k}\frac{1}{z^n} \tag{46}$$

where $\mathrm{Li}_k(z)$ is the k*th* polylogarithm function.[20] $\mathrm{Li}_k(1/z)$ has exactly the same analytic structure as $\ln(1-1/z)$ and in fact $\ln(1-1/z) = \mathrm{Li}_1(1/z)$.

If there *were* discrete eigenvalues away from the real axis, then the $b_{n,s}$ would have to have an oscillatory behavior as a function of n; indeed, it would have to have an infinite number of oscillations in n. The basic idea is that such behavior could occur only if $\rho(x)$ itself had oscillations on all scales, which is impossible for an analytic function.

It remains possible that, for instance, $b_{n,s}$ may have a component proportional to $2^{-n}/n$ or some other mixture of exponential and power-law dependence on n. In that case $\beta_s(z)$ will still have a branch point at $z = 0$. As one moves away from $z = 0$ the structure could become more complicated; there might conceivably be a whole set of branch points and poles. superimposed along each other along the $[0, 1]$. Fortunately, a great deal can be found from just main branch cut. In particular it can give information about the large t behavior of correlation functions.

3.2. The *x* – *x* Autocorrelation for the Cusp Map

Even partial knowledge about $\beta_s(z)$ (or, equivalently, $b_{n,s}$) can give useful information about the long-time evolution of densities. The rule is

that the dominant large n behavior of $b_{n,s}$ determines the dominant large t evolution of densities.

In particular, one can easily find the leading contribution to the $x-x$ autocorrelation function:

$$C(t) = \lim_{T\to\infty} \frac{1}{T} \sum_{\tau=0}^{T-1} x_\tau (x_{\tau+t} - \bar{x}) \tag{47}$$

With some additional work, corrections to the leading contribution to $C(t)$ can also be calculated.

Since the cusp map is ergodic,[18]

$$\begin{aligned} C(t) &= \langle x \mid U^t(x\rho^{\text{eq}})\rangle - \langle x \mid x\rho^{\text{eq}}\rangle \\ &= \langle x \mid U^t\, \delta\rho\rangle \end{aligned} \tag{48}$$

where $\delta\rho(x) = x\rho^{\text{eq}} - \frac{1}{3}\rho^{\text{eq}}(x)$. The expansion of $C(t)$ in terms of the smooth coherent states is

$$\begin{aligned} C(t) &= \int_0^1 x U^t\, \delta\rho(x)\, dx \\ &= \frac{1}{2\pi i} \sum_{s=1}^{\infty} \int_0^1 x \oint_{|z|=1} z^t \beta_s(z)\, \psi_{z,s}(x)\, dz\, dx \end{aligned} \tag{49}$$

We now find the dominant large-n behavior of the $b_{n,s}$ and the corresponding components of the $\beta_s(z)$. The expansion coefficients are from (38):

$$\begin{aligned} b_{n,s} &= \int_0^1 \tilde{g}^0_{n,s}(x)\, \delta\rho(x)\, dx \\ &= \int_0^1 \tilde{g}_{n,s}(x)\, \delta\rho(x)\, dx \\ &\approx \int_0^{\xi^0_n} \tilde{g}_{n,s}(x)\, \delta\rho(x)\, dx \end{aligned} \tag{50}$$

We can replace $\tilde{g}^0_{n,s}(x)$ by $\tilde{g}_{n,s}(x)$ inside the integral since they only differ by a constant and $\delta\rho(x)$ integrated over any constant is zero. The approximation in the last step is valid for n large and is made because $\delta\rho(1) = 0$ and the integrand oscillates extremely rapidly away from the endpoints of the unit interval. Neglected contributions decrease as $1/n^2$ or faster.

Carrying on we have

$$\begin{aligned} b_{n,s} &\approx \delta\rho(0) \int_0^{\xi_n^0} [\tilde{g}_{n,s}(x) + k_s]\, dx, \qquad n \text{ large} \\ &= \delta\rho(0)\, k_s \xi_n^0 \\ &\approx -\frac{2}{3} k_s \frac{2}{n+9} \left(1 - \frac{\ln n}{n+1}\right) \end{aligned} \tag{51}$$

where the higher-order approximation to ξ_n^0 is based on the continuous-time approximation.[15] The approximation in (51) is valid up to $\ln n/n^2$. Call the two components of $b_{n,s}$ above in (51) $b_{n,s}^{(1)}$ and $b_{n,s}^{(2)}$:

$$b_{n,s}^{(1)} = -\frac{4}{3} \frac{k_s}{n+9} \tag{52}$$

$$b_{n,s}^{(2)} = \frac{4}{3} \frac{k_s}{n+9} \frac{\ln n}{n+1} \tag{53}$$

with corresponding components of $\beta_s(z)$:

$$\beta_s^{(1)}(z) = \sum_{n=0}^{\infty} b_{n,s}^{(1)} z^{-(n+1)} \tag{54}$$

$$\beta_s^{(2)}(z) = \sum_{n=0}^{\infty} b_{n,s}^{(2)} z^{-(n+1)} \tag{55}$$

The leading contribution to $C(t)$ is

$$\begin{aligned} C^{(1)}(t) &= \frac{1}{2\pi i} \sum_{s=1}^{\infty} \int_0^1 x \oint_{|z|=1} z^t \sum_{n=0}^{\infty} b_{n,s}^{(1)} z^{-(n+1)} \psi_{z,s}(x)\, dz\, dx \\ &\approx 0.39269 \frac{1}{t} - 1.6584 \frac{\ln t}{t^2} \end{aligned} \tag{56}$$

where details of the calculation are given in the Appendix.

Another correction to $C(t)$ of order $\ln t/t^2$ comes from $b_{n,s}^{(2)}$, given in (53). That component yields a correction $C^{(2)}(t)$, defined exactly analogously to $C^{(1)}(t)$:

$$\begin{aligned} C^{(2)}(t) &= \frac{1}{2\pi i} \sum_{s=1}^{\infty} \int_0^1 x \oint_{|z|=1} z^t \sum_{n=0}^{\infty} b_{n,s}^{(2)} z^{-(n+1)} \psi_{z,s}(x)\, dz\, dx \\ &\approx -0.39269 \frac{\ln t}{t^2} \end{aligned} \tag{57}$$

where details of the calculation are also given in the Appendix.

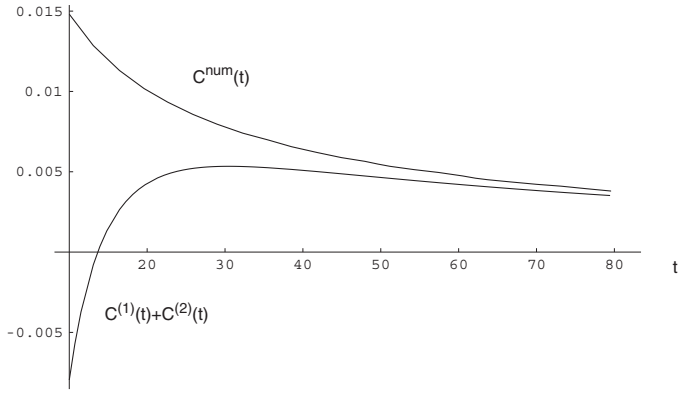

Fig. 6. The upper curve, $C^{\text{num}}(t)$, is the result of calculating the integral (62) numerically. The lower curve is $C^{(1)}(t)+C^{(2)}(t) = 0.39269/t - 2.0511 \ln t/t^2$.

Combining $C^{(1)}(t)$ and $C^{(2)}(t)$, one finds a large-t approximation to $C(t)$ is

$$C(t) \approx 0.39269 \frac{1}{t} - 2.0511 \frac{\ln t}{t^2} \tag{58}$$

which should be valid up to $\ln t/t^2$. Figure 6 shows a comparison of the above result to values of $C(t)$ that were calculated numerically directly from the integral expression

$$C(t) = \int_0^1 K^t[x]\, \delta\rho(x)\, dx \tag{59}$$

Obviously the fit is good for even moderately high values of t. The sort of approximation in (58) is especially useful because the direct numerical approach to finding $C(t)$ is quite difficult for t as low as 10 and is extremely difficult to extend past $t = 100$ with much accuracy.

The $1/t$ term in $C(t)$, which is dominant for large t, yields a frequency spectral density of

$$S(\omega) \equiv \sum_{t=0}^{\infty} \cos \omega t\, C(t) \tag{60}$$

having a dominant term for small ω of

$$S(\omega) \propto -\ln \omega \tag{61}$$

The result in (58) is an extension of certain results in Ref. 15, in which the functional form of both the leading contribution to $C(t)$ and the first correction was found, but a less accurate approximation was used to obtain their weights.

4. EXTENSION TO OTHER MAPS

The technique described here is applicable to other one-dimensional maps with marginal fixed points, such as the Farey map[17] and the Manneville–Pomeau map.[4] For any map $f(x)$ with a marginal fixed point at x_0, the branch of $f^n(x)$ containing x_0 will have a length that decreases slower than exponentially as a function of n. That is the key feature allowing the construction of smooth coherent states to work.

Certain modifications may be necessary, for instance to deal with the Farey map's singular invariant density. For maps that are even around their midpoint, dual shift states can be found just as for the cusp map. For maps that lack clear symmetry, the dual shift states will be harder to find. If necessary, a set of them can be found numerically at the cost of introducing another layer of approximation.

It is clear that for any map to which the technique is applicable at all, imposing a differentiability condition on densities does not reduce the spectrum of U to anything less than the unit disk. The effect of imposing the condition of analyticity is less clear, but we conjecture that for a wide class of intermittent maps the effect is the same as for the cusp map: The spectrum of U is reduced to real $z \in [0, 1]$.[19]

5. CONCLUSION

The statistical dynamics of a deterministic system is contained entirely in its Frobenius–Perron operator. For systems with exponential approach to equilibrium this operator has discrete decay modes that characterize the details of the approach. Power-law decay may be decomposed into a continuum of exponentially decaying contributions. We have shown a way to calculate such exponential decay modes and express the power law decay in terms of them for a class of systems using a coherent state technique.

This technique has been applied to the well-known cusp map to yield smooth exponentially decaying eigenstates. The $x - x$ autocorrelation was then calculated using these states and shown to decay with a dominant power-law time dependence of t^{-1} corrected by a term with $t^{-2} \ln t$ behavior.

Our technique serves as an alternative to other analyses of non-exponential time dependence. The idea can be applied to other systems with non-exponential decay, including those with singular invariant densities.

APPENDIX

This Appendix presents calculations for the leading-order terms in the $x-x$ autocorrelation $C(t)$ for large t.

The leading contribution to $C(t)$ is given by

$$C^{(1)}(t) = \frac{1}{2\pi i} \sum_{s=1}^{\infty} \int_0^1 x \oint_{|z|=1} z^t \sum_{n=0}^{\infty} b_{n,s}^{(1)} z^{-(n+1)} \psi_{z,s}(x)\, dz\, dx \tag{62}$$

Now, k_s, and hence $b_{n,s}$, should depend on s as $1/s$. The integral of $x\psi_{z,s}(x)$ over x should have the same s dependence. So the terms in the sum above should decrease with s as $1/s^2$. In fact, numerical work shows that they decrease even faster than that for small s. So it it is a good approximation to keep only $s=1$ in the above sum. (In any case, keeping the full sum in s would not alter the t dependence of the terms in $C(t)$ to be found below. Only the weights of the various terms would be altered.)

$$\begin{aligned} C^{(1)}(t) &\approx \frac{1}{2\pi i} \int_0^1 x \oint_{|z|=1} z^t \sum_{n=0}^{\infty} b_{n,1}^{(1)} z^{-(n+1)} \psi_{z,1}(x)\, dz\, dx \\ &= -\frac{4}{3} k_1 \frac{1}{2\pi i} \int_0^1 x \oint_{|z|=1} z^t \sum_{n=0}^{\infty} \frac{z^{-(n+1)}}{n+9} \psi_{z,1}(x)\, dz\, dx \\ &= -\frac{4}{3} k_1 \frac{1}{2\pi i} \int_0^1 x \oint_{|z|=1} z^t z^8 \left[-\sum_{n=1}^{8} \frac{z^{-n}}{n} + \ln(1-1/z) \right] \psi_{z,1}(x)\, dz\, dx \end{aligned} \tag{63}$$

The first term in brackets can be dropped because when multiplied by z^8 it is a polynomial, so its contour integral around a closed path is 0. Next deform the contour to run right around the branch cut in $\ln(1-1/z)$ between $z=0$ and $z=1$, so the complex variable z can be replaced by the real variable y:

$$\begin{aligned} & C^{(1)}(t) \\ & \approx -\frac{4}{3} \frac{k_1}{2\pi i} \int_0^1 x \int_0^1 y^{t+8} \left\{ \left[\ln \left| 1 - \frac{1}{y} \right| + \pi i \right] - \left[\ln \left| 1 - \frac{1}{y} \right| - \pi i \right] \right\} \psi_{y,1}(x)\, dy\, dx \\ & = -\frac{4}{3} k_1 \int_0^1 x \int_0^1 y^{t+8} \psi_{y,1}(x)\, dy\, dx \\ & = -\frac{4}{3} k_1 \int_0^1 y^{t+8} \sum_{m=0}^{\infty} y^m \int_0^1 x g_{m,1}(x)\, dx\, dy \\ & = -\frac{4}{3} k_1 \sum_{m=0}^{\infty} \frac{w_{m,1}}{m+t+8} \end{aligned} \tag{64}$$

where

$$w_{m,s} \equiv \int_0^1 x g_{m,s}(x)\, dx \tag{65}$$

For values of m that are not too high (up to about 50), it is possible to calculate $w_{m,1}$ numerically fairly easily. For higher values of m it is possible to obtain a fairly good approximation. First note that all the $g_{m,1}(x)$ have the same basic shape as those shown in Fig. 2; they merely become more and more compressed with increasing m. Using the continuous-time approximation again,[15] it can be shown that the maximum and minimum of $g_{m,1}(x)$ are both at $2/(m+m_o)$ for some m_o, with the expression becoming exact in the limit of large m. Numerically it is found that for the maximum, $m_o = 11.7$ and for the minimum $m_o = 8.5$. Also note that the point where the graph of $g_{m,1}(x)$ crosses the x-axis is exactly ξ^0_m, and the maximum of the support of $g_{m,1}(x)$ is ξ^0_{m-1}. So:

$$\begin{aligned} w_{m,1} &\approx \frac{2}{m+11.7}\int_0^{\xi^0_m} g_{m,1}(x)\, dx + \frac{2}{m+8.5}\int_{\xi^0_m}^{\xi^0_{m-1}} g_{m,1}(x)\, dx \\ &= \frac{2}{m+11.7}\int_0^{1/2} g_{0,1}(x)\, dx + \frac{2}{m+8.5}\int_{1/2}^1 g_{0,1}(x)\, dx \\ &= 2\left(\frac{1}{m+11.7} - \frac{1}{m+8.5}\right)\int_0^{1/2} g_{0,1}(x)\, dx \\ &\approx -\frac{4.07437}{(m+8.5)(m+11.7)} \end{aligned} \tag{66}$$

where the first step follows from the fact $g_{m,1}(x) = U_0^{-m} g_{0,1}(x)$ and U_0^{-1} preserves the integral over x of any function it is applied to. The integral of $g_{0,1}(x)$ was done numerically.

Call the approximation in (66) $\tilde{w}_{m,1}$. Now we are in a position to find the dominant large t behavior of $C^{(1)}(t)$. Look at (64) and note that each individual term has a large t dependence proportional to $1/t$. Since the $w_{m,1}$ themselves decrease quickly, to leading order in t we can replace $1/(m+t+8)$ by $1/t$. The result is

$$\begin{aligned} C^{(1)}(t) &\approx -\frac{4}{3} k_1 \sum_{m=0}^{\infty} w_{m,1} \frac{1}{t} \\ &\approx 0.39269 \frac{1}{t} \end{aligned} \tag{67}$$

where for m up to 30, $w_{m,1}$ was evaluated numerically and for higher m the approximation $\tilde{w}_{m,1}$ was used, giving an infinite sum that could be evaluated analytically. k_1 was also found numerically.

One can also find a component of $C^{(1)}(t)$ that represents a higher-order correction to the above. To that order, it is accurate to start out by replacing all $w_{m,1}$ by $\tilde{w}_{m,1}$ in (64). The infinite sum in that can then be done analytically. It will yield a term in $1/t$ (already dealt with), a term in $1/t^2$ (which could be dealt with, but will be neglected), plus the following term:

$$-\frac{4}{3}k_1\frac{263.70\,\psi(t+8)}{(1+\sqrt{5}\,)(2t-1)(10t-37)}\approx -1.6584\,\frac{\ln t}{t^2},\qquad t \text{ large} \tag{68}$$

where $\psi(t)$ is the digamma function $\psi(t)=\Gamma'(t)/\Gamma(t)$.[20]

$C^{(2)}(t)$, defined in (57), is yet a further correction.

$$\begin{aligned}C^{(2)}(t) &= \frac{1}{2\pi i}\sum_{s=1}^{\infty}\int_0^1 x\oint_{|z|=1} z^t \sum_{n=0}^{\infty} b^{(2)}_{n,s} z^{-(n+1)}\psi_{z,s}(x)\,dz\,dx\\ &\approx \frac{4}{3}k_1\frac{1}{2\pi i}\int_0^1 x\oint_{|z|=1} z^t \sum_{n=0}^{\infty}\frac{\ln n}{(n+9)(n+1)} z^{-(n+1)}\psi_{z,1}(x)\,dz\,dx\\ &\approx \frac{4}{3}k_1\frac{1}{2\pi i}\int_0^1 x\oint_{|z|=1} z^t \sum_{n=0}^{\infty}\frac{\ln n}{n^2} z^{-(n+1)}\psi_{z,1}(x)\,dz\,dx\end{aligned} \tag{69}$$

where as before only $s=1$ is retained and in the second step the approximation $1/[(n+9)(n+1)]\approx 1/n^2$ is used, an approximation with an error that goes as $1/n^3$ and hence that can be ignored to the accuracy with which we are working. The sum above can be done analytically, yielding

$$C^{(2)}(t)\approx \frac{4}{3}k_1\frac{1}{2\pi i}\int_0^1 x\oint_{|z|=1} z^t\lambda_2(1/z)\,\psi_{z,1}(x)\,dz\,dx \tag{70}$$

where

$$\lambda_\alpha(z)\equiv\frac{\partial}{\partial\alpha}\mathrm{Li}_\alpha(z) \tag{71}$$

$\lambda_2(1/z)$ has a branch cut running between $z=0$ and $z=1$. As before, deform the contour to run around that branch cut:

$$C^{(2)}(t)\approx \frac{4}{3}k_1\frac{1}{2\pi i}\int_0^1 x\int_0^1 y^t\left[\mathrm{Im}\,\lambda_2\!\left(\frac{1}{y-i\epsilon}\right)-\mathrm{Im}\,\lambda_2\!\left(\frac{1}{y+i\epsilon}\right)\right]\psi_{y,1}(x)\,dy\,dx \tag{72}$$

where the real parts of $\lambda_2(1/z)$ above and below the cut cancel out. The imaginary parts above and below are negatives of each other:

$$C^{(2)}(t) \approx \frac{4}{3} k_1 \frac{2}{2\pi i} \int_0^1 \int_0^1 y^t \operatorname{Im} \lambda_2(1/y)\, \psi_{y,1}(x)\, dy\, dx \tag{73}$$

where the branch cut is now regarded as displaced infinitesimally above the real axis.

$$C^{(2)}(t) \approx \frac{4}{3} k_1 \frac{1}{\pi i} \sum_{m=0}^{\infty} \int_0^1 x g_{m,1}(x)\, dx \int_0^1 y^{m+t} \operatorname{Im} \lambda_2(1/y)\, dy \tag{74}$$

It can be shown analytically from the properties of $\lambda_2(z)$ that the integral over y approaches $\pi \ln t/t^2$ for large t, so

$$C^{(2)}(t) \approx \frac{4}{3} k_1 \frac{1}{\pi i} \sum_{m=0}^{\infty} w_{m,1} \pi \frac{\ln t}{t^2} \tag{75}$$

Once the sum over m is dealt with as before, by finding $w_{m,1}$ numerically for m up to 60 and using the approximation $\tilde{w}_{m,1}$ for higher m, we obtain

$$C^{(2)}(t) \approx -0.39209 \frac{\ln t}{t^2} \tag{76}$$

ACKNOWLEDGMENTS

We thank I. Prigogine for his support and encouragement. We acknowledge the suggestions of H. H. Hasegawa and comments on our manuscript from Brian LaCour, Chun-Biu Li, and Gonzalo Ordóñez. This work was supported by the Engineering Research Program of the Office of Basic Energy Sciences at the U.S. Department of Energy, Grant DE-FG03-94ER14465, the Robert A. Welch Foundation Grant F-0365, and the European Commission Contract ESPRIT Project 28890 (CTIAC), Communauté francaise de Belgique, and the "Loterie Nationale" of Belgium.

REFERENCES

1. M. Schroeder, *Fractals, Chaos, Power Laws* (W. H. Freeman, New York, 1991). D. Sornette, *Critical Phenomena in Natural Sciences* (Springer-Verlag, Berlin, 2000).
2. P. Bak, C. Tang, and K. Wiesenfeld, Self-organized criticality: An explanation of $1/f$ noise, *Phys. Rev. Lett.* **59**:381–384 (1987).

3. E. Weeks, T. Solomon, J. Urbach, and H. Swinney, Observations of anomalous diffusion and Lévy flights, in *Lévy Flights and Related Topics in Physics*, M. Shlesinger, G. Zaslavsky, and U. Frisch, eds. (Springer-Verlag, Berlin, 1995).
4. P. Manneville, Intermittency, self-similarity and $1/f$ spectrum in dissipative dynamical systems, *J. Physique* **41**:1235–1243 (1980). Y. Pomeau and P. Manneville, Intermittent transition to turbulence in dissipative dynamical systems, *Comm. Math. Phys.* **74**:189–197 (1980).
5. H. G. Schuster, *Deterministic Chaos* (VCH Publishers, Weinheim, 1988).
6. A. Lasota and M. C. Mackey, *Chaos, Fractals and Noise* (Springer-Verlag, New York, 1994).
7. D. J. Driebe, *Fully Chaotic Maps and Broken Time Symmetry* (Kluwer Academic Publishers, Dordrecht, 1999).
8. P. Gaspard, *Chaos, Scattering and Statistical Mechanics* (Cambridge University Press, Cambridge, 1998).
9. I. Antoniou and G. Lumer, eds., *Generalized Functions, Operator Theory, and Dynamical Systems* (Chapman & Hall/CRC Press, Boca Raton, 1999).
10. D. Ruelle, Resonances of chaotic dynamical systems, *Phys. Rev. Lett.* **56**:405–409 (1986).
11. A. Van Der Ziel, On the noise spectra of semi-conductor noise and of flicker effect, *Phys.* **16**:359–372 (1950).
12. W. Saphir and H. Hasegawa, Spectral representations of the Bernoulli map, *Phys. Lett. A* **171**:317–322 (1992). I. Antoniou and S. Tasaki, Spectral decomposition of the Renyi map, *J. Phys. A* **26**:73–94 (1993). E. C. G. Sudarshan, Coherence and chaos, in *Coherent States: Past Present and Future* (World Scientific Publishing, 1994).
13. H. H. Hasegawa and E. Luschei, Exact power spectrum for a system of intermittent chaos, *Phys. Lett A* **186**:193–202 (1994).
14. Z. Kaufman, H. Lustfeld, and J. Bene, Eigenvalue spectrum of the Frobenius–Perron operator near intermittency, *Phys. Rev. E* **53**:1416–1421 (1996).
15. S. Grossman and H. Horner, Long time tail correlations in discrete chaotic dynamics, *Z. Phys. B* **60**:79–85 (1985).
16. P. Collet and S. Isola, On the Essential Spectrum of the Transfer Operator for Expanding Markov Maps, *Comm. Math. Phys.* **139**:551–557 (1991).
17. M. J. Feigenbaum, Presentation functions, fixed points, and a theory of scaling function dynamics, *J. Statist. Phys.* **52**:527–569 (1988).
18. P. C. Hemmer, The exact invariant density for a cusp-shaped return map, *J. Phys. A* **17**:L247–L249 (1984). G. Györgyi and P. Szépfalusy, Fully developed chaotic 1-d maps, *Z. Phys B* **55**:179–186 (1984).
19. H. H. Rugh, Intermittency and regularized Fredholm determinants, *Invent. Math.* **135**:1–24 (1999).
20. J. Spanier and K. B. Oldham, *An Atlas of Functions* (Hemisphere Publishing Corporation, New York, 1987).
21. A. Ben-Mizrachi, I. Procaccia, N. Rosenberg, A. Schmidt, and H.G. Schuster, Real and apparent divergencies in low-frequency spectra of nonlinear dynamical systems, *Phys. Rev. A* **31**:1830–1840 (1985).